IPTC-20061-Abstract

A Hydrocarbon Production System Multi-Objective Optimization

Joseph Rizzo Cascio, Eni S.p.A.; Francesco Di Maio, Politecnico di Milano; Amalia Bianco, Sergio Ritondale, Luca Cadei, and Marco Montini, Eni S.p.A.; Fabio Rinaldi, Enrico Zio, and Behzad Najafi, Politecnico di Milano

This paper was prepared for presentation at the International Petroleum Technology Conference held in Dhahran, Saudi Arabia, 13 – 15 January 2020.

Abstract

The benefits of a multi-objective optimization approach embedding an accurate exergy model of a hydrocarbon production system are shown on a real oil and gas facility. The innovative tool developed is based on a biogenetical differential evolution algorithm, which exploits a self-adaptive iterative procedure to maximize the value of the Asset. The optimization integrates the production system considering the trade-off between hydrocarbon production, energy consumption and efficiency. The Asset value optimization is one of the most complex and multi-disciplinary task in the oil and gas industry, due to the high number of objectives and their synergy. An integrated physical model of wells, gathering network and process plant is built and, then, used for exergy efficiency and gas production optimization. Conflicts and interactions among process variables and operational constraints are treated and solved holistically by the tailored evolutionary algorithm. This has also been integrated with a quick and efficient exergetic and thermoeconomic analysis in order to grant the achievement of the maximum asset value. The multi-objective optimization provides a trade-off between the optimal values of exergy efficiency and gas production that would have been obtained independently with single-objective optimizations. In fact, the exergy efficiency optimization is driven towards a configuration having lower irreversibilities: by apportioning the entire system exergy into the exergy destroyed by each piece of equipment and by calculating its local efficiency, the most contributing to irreversibility generation is identified. Moreover, the exergy analysis is complemented with an exergetic and a thermoeconomic cost analysis: the exergy analysis, apart from describing the quality of any thermodynamic process, does not give any information about the costs of each system stream, which can be even more interesting and of practical application. Indeed, the exergy analysis is proven to be an accurate way of assessing which equipment is performing worse. Therefore, it leads to preventive corrective actions to ensure good thermodynamic performance of the system and supports the decision process in the choice of maintenance operations. The thermoeconomic analysis, based on the theory of exergetic costs, confirms the improved management of the process plant and its efficiency enhancement, without neglecting the main target of the oil and gas industries that is production maximization. The benefits of a novel multi-objective biogenetical approach to solve and optimize a hydrocarbon production system in terms of exergy efficiency and gas production are shown, with respect not only to other methodologies of literature but also

in terms of exergetic and thermoeconomic costs of the solutions provided, allowing to achieve the highest value of the operated asset.

Introduction

The global energy scenario is continuously changing and traditional centres of demand are being overtaken by fast-growing emerging markets. Until now, considerable progress has been made, but there is still a long way to go if we want to continue to meet the energy needs of a changing world. This makes the overall energy demand continuously expanding unless limited by improvements in energy production and conversion [BP Energy Outlook, 2017]. In this scenario, the oil and gas industry plays a fundamental role, since it still endorses most of the energy production and reaches the best energy conversion efficiency among the other possible alternatives. The oil and gas industries are challenged by the capability of optimally define the operational settings (e.g., choke status, separator pressure, reboiler temperature, etc.) of the production system that consists in one or more reservoirs and wells connected with the production facilities by a gathering network of pipelines. The reservoir supplies the wellbore with hydrocarbons (mainly crude oil and/or gas) and other non-hydrocarbon fluids, thanks to the pressure difference between the reservoir and the surface. The well, through tubing, provides a path for the production fluids to flow from the bottom-hole to the well-head and offers a means to control the rate simply operating on the surface choke that regulates the flow rate of hydrocarbons extracted from the reservoir. Then, the pipeline network gathers the production fluids to the process facilities. The optimization of the production system is a complex multidisciplinary problem: specifically, the gathering is driven by fluid mechanics principles (the reservoir pressure drives the fluids to the surface and then by pipelines to the delivery or process area; artificial lift methods are often applied between the pressure source and the delivery point to add pressure energy to the system), whereas the process is required to meet physical and chemical specifications, for the sake of the finite product quality. This complex non-linear optimization problem has encouraged Eni S.p.A. to develop an in-house optimization tool [G. Viadana et al., 2012], [G. Viadana et al., 2013] that optimizes the production system, combining subsurface models, surface production facilities and engineering/processing models [F. Verre et al., 2011], [S. Scaramellini et al., 2015], [S. Scaramellini et al., 2017], [S. Brioschi et al., 2017]. This tool is an evolutionary algorithm that solves single-objective optimization problems. However, multi-objective optimization algorithms become mandatory when addressing a multidisciplinary problem (with conflicting objectives) such as the management of oil and gas production systems. Gas production and plant exergy efficiency are, indeed, conflicting objectives. For instance, considering a stream of hydrocarbons entering a generic separator, the optimal value of separator pressure that maximizes the production of gas is the lowest as possible (i.e., free gases release is favoured), although this requires more energy to compress the produced gas up to the delivery pressure level dictated by specifications, which, hence, increases resource consumption. In this paper, a novel multi-objective approach is proposed that consists of a Multi-Objective Differential Evolution (MODE) algorithm. This simultaneously accounts for several objectives to ensure good performance in terms of convergence speed, results accuracy, distribution and spread of the obtained Pareto optimal front. Among all, the implementation of a novel mutation strategy represents its main feature that ensures good performance throughout the evolution process. A real-case application of the multi-objective optimization tool is, then, shown with the purpose of proving the benefits of the proposed approach with respect to other methodologies of literature, in terms of exergetic and thermoeconomic costs. The two objectives to be optimized are gas production and exergy efficiency of the plant: on one hand, the significant amount of gas produced by the field under investigation and in the perspective of its increasing gas/oil ratio, gas production optimization is a crucial aspect for Eni S.p.A. interests; on the other hand, the optimization of the thermodynamic quality throughout the treatment of hydrocarbons requires optimizing the exergy efficiency of the processes needed.

Statement of Theory and Definitions

Let us consider a generic optimization problem with M objectives subjected to C constraints, denoted as h_c, c = 1, 2, …, C. The decision variables of the optimization problem are n real variables x_j, j = 1, 2, …, n, defined as:

$$x_j \in \left[x_j^L,\ x_j^U\right] \tag{1}$$

where xjL and xjU are the lower and upper bound, respectively. Any possible set of these variables x¯=(x1,x2, …, xn): x¯∈D⊆ℝN is a solution inside the variables search space D, with corresponding objective functions values:

$$f_m(\bar{x}) = f_m(x_1, x_2, \ \ldots,\ x_n),\ m = 1,\ 2,\ \ldots,\ M \tag{2}$$

Constraints limit D to the feasible region Ω⊆D, within which the optimal set of feasible variables values that satisfies the optimization problem can be found:

$$\bar{x}^* = \left(x_1^*, x_2^*,\ \ldots,\ x_n^*\right):\ \ \bar{x}^* \in \Omega \subseteq D \tag{3}$$

When the optimization goal is to minimize a single objective f_m, the task (in the case of a minimization problem) is to find:

$$\bar{x}^* \big| \ f_m(\bar{x}^*) < f_m(\bar{x}) \ \ \forall \ \ \bar{x} \in \Omega \tag{4}$$

Whereas, in case of optimization of two or more conflicting objectives, the optimization target is a vector of objective functions:

$$\bar{F}(\bar{x}) = \left(f_1(\bar{x}), f_2(\bar{x}),\ \ldots,\ f_m(\bar{x})\right) \in R^M \tag{5}$$

The problem can be formulated defining two operators, ≻ and ≢, that are related to the concept of dominance. Assuming two feasible solutions, x¯1 and x¯2, we say that they are different (≢) if:

$$\bar{x}^1 \not\equiv \bar{x}^2 \text{ if } \exists\, x_j^1 \in \bar{x}^1, x_j^2 \in \bar{x}^2 \big| \ x_j^1 \neq x_j^2 \tag{6}$$

We say that x¯1 is dominated by x¯2 (≻) if:

$$\bar{x}^1 \succ \bar{x}^2 \text{ if } \forall\, x_j^1 \in \bar{x}^1, x_j^2 \in \bar{x}^2 \big| \ \ \bar{x}^1 \leq \bar{x}^2 \text{and } x_j^1 \neq x_j^2 \tag{7}$$

A set of non-dominated (equally good) solutions (called Pareto optimal set) is found, within which each solution cannot be said to be better or worse than others if:

$$\bar{x}^* \in \Omega \text{ if } \nexists\, \bar{x} \in \Omega \ \ \bar{F}(\bar{x}) \succ \bar{F}(\bar{x}^*) \tag{8}$$

In [S. Bandyopadhyay et al., 2013] a broad survey of optimization techniques is provided, including Genetic Algorithms ([D. E. Goldberg, 1989], [J. H. Holland, 1975], [L. Chambers, 1995]) Differential Evolution ([R. Storn et al., 1997]) and Particle Swarm Optimization ([J. Kennedy, 2011]), to cite a few. The developed novel algorithm is a multi-objective optimization tool aiming at finding the Pareto optimal front of a set of objective functions F¯(x¯) of one or more optimization variables x¯=(x1,x2, …, xn). The conceptual core is a Differential Evolution algorithm (DE), whose mutation strategy has been tailored to the optimization problem. DE represents a branch of evolutionary algorithms developed for optimization problems over continuous domain and apply evolution operations on the individuals of the population to perturb them by transmission of good properties and find the final optimum of the system [R. Storn et al., 1997]. One of the key points of DE is that the value of each optimization variable in the individual is represented by a real number. A classic DE accounts for the following steps:

1. parameters setting and creation of an initial population of NP (number of individuals in the population) potential solutions to the problem;

2. evaluation of their fitnesses (objective functions);
3. for each target vector, selection of three individuals for reproduction;
4. for each target vector, creation of noisy vector using the mutation process;
5. creation of a trial vector, mixing target and noisy vectors;
6. comparison between each target vector and its related trial, and in case replacement;
7. control for the stopping criteria:
   - if some criterion is met, then stop;
   - else go to step 3.

The DE mutation process accounts for a single mutation operator throughout the evolution process; in this thesis, we propose a novel algorithm implementing a mutation strategy, as follows: a single mutation operator based on random individuals selection (i.e., DE/rand/1) is used to produce the candidate solutions at the early stage of the evolution, whereas a mutation strategy that chooses between two alternative mutation operators is employed at the later phases of the evolution to generate offsprings. The main reason for this is that some greedy mutation operators may reduce the population diversity in the early stage of the evolution, endangering the capability of solving multi-objective optimization problems [Q. Fan et al., 2015], [Q. Fan et al., 2017]. Thus, two mutation operators (i.e., DE/rand/1 and DE/best/1) are utilized: the former has good exploration search capability, whereas the latter is good at local searching and its convergence is faster than that of DE/rand/1. Therefore, combining in a suitable way these mutation operators in a single strategy can provide improved search capabilities during the evolutionary process by maintaining the population diversity in the early stages of the search, while reducing the computational complexity of the algorithm during the entire evolutionary process. The mutation strategy can be fully controlled operating on two control parameters: the percentage factor g and the mutation pressure q. The first is the fraction of the maximum number of generations, denoted as G*, in which only the DE/rand/1 mutation operator is applied and, then, the DE/best/1 mutation operator can be randomly used accordingly to the probability $0 \leq q \leq 1$:

$$\text{random}[0, \quad 1] = \begin{cases} > q \quad DE/rand/1 \quad is \quad applied \\ \leq q \quad DE/best/1 \quad is \quad applied \end{cases} \tag{9}$$

where random[0, 1] stands for a uniform random value sampled between 0 and 1. The selection of the final optimal solution from the Pareto front depends on the preferences and criteria of the decision maker on the different, multiple objectives. In this work, the TOPSIS technique (Technique for Order of Preference by Similarity to Ideal Solution) is used as it only requires the scaling of all the objectives to be implemented, allowing to quickly identify the final optimal solution [M. Aminyavari et al., 2016], [P. Baraldi et al., 2016]. Indeed, after scaling of each objective function, two points are defined: the ideal and non-ideal points. The ideal point collects the best values of each objective function obtained separately, without fulfilling the other objectives, representing a fictitious point in the objective space. The non-ideal point, on the other hand, collects the worst values of each objective obtained separately, again without fulfilling the other objectives, hence, representing another fictitious point in the objective space. The TOPSIS technique finds the final optimal point as the one having the shortest possible distance from the ideal point and the farthest possible distance from the non-ideal one. In conclusion, a final check procedure on the obtained Pareto optimal front to eliminate all the non-dominated solutions having the same values of decision variables is implemented. Notice that, another technique is implemented to randomly extract the best current individual. It consists of a non-dominated sorting of the current population at each generation G to store the non-dominated solutions in a temporary pool, from which a randomly extracted one as best individual of the current population at generation G, represents the base vector for the DE/best/1 mutation operator. The multi-objective optimization tool is tested against some already acknowledged multi-objective optimization algorithms, namely:

- the Multi-Objective Differential Evolution (MODE) [T. Robič et al., 2005], [B. V. Babu et al., 2007];
- the Multi-Objective Genetic Algorithm (MOGA) [T. Murata et al., 1995], [A. Konak et al., 2006]:
- the fast elitist multi-objective Non-dominated Sorting Genetic Algorithm (NSGA-II) [K. Deb et l., 2002], [A. Seshadri, 2007].

All these algorithms have been tuned to be tested on a known test function. Thus, an artificially constructed test function named ZTD1 [E. Zitzler et al., 2000] is adopted as it allows easy implementation, easy visualization and known optima in advance [T. Sağ et al., 2016]. ZTD1 has a convex Pareto optimal front, n = 30 with *x_i#[0, 1]* and its objective functions are:

$$f_1(x_1) = x_1 \tag{10}$$

$$f_2(\bar{x}) = g(x_2, \quad \ldots, \ x_n) \cdot h(f_1(x_1), \ g(x_2, \quad \ldots, \ x_n)) \tag{11}$$

where:

$$g(x_2, \quad \ldots, \ x_n) = 1 + 9 \cdot \sum_{i=2}^{n} \frac{x_i}{n-1} \tag{12}$$

$$h(f_1, \ g) = 1 - \sqrt{\frac{f_1}{g}} \tag{13}$$

The Pareto optimal front is formed with g(x¯)=1. The test has been carried out fixing the values of population size NP and maximum number of generations G_{MAX}, this latter representing the stopping criterion, as in Table 1.

Table 1—Evolution setting

Parameter	Value
NP	200
G_{MAX}	500

The default values set for the novel algorithm parameters, derived by a trial and error procedure, have also been adopted for the other benchmarking problems, which, accidentally, correspond to their MATLAB default settings, as reported in Table 2.

Table 2—Algorithm parameter settings

Novel algorithm	
Parameter	Value
CR_C	0.5
F_C	0.5
q	0.5
g	0.2

MODE	
Parameter	Value
CR	0.5
F	0.5

MOGA	
Parameter	Value
CR	0.5
EC	$0.5 \cdot NP$
PF_f	1

NSGA-II	
Parameter	Value
CR	0.5
m_p	0.1

We indicate with CR the crossover rate and with F the scaling factor and, in the novel algorithm, their evolution as generations proceed is ruled by CR_C (i.e., crossover rate threshold) and F_C (i.e., scaling factor threshold), respectively. In MOGA, we use EC for the elite count (i.e., the number of best individuals that survive to the next generation without any change) and PF_f for the Pareto front fraction (i.e., fraction of population on non-dominated front), while in NSGA-II, m_p stands for the mutation probability. To compare these algorithms rigorously (or to measure the performance of a multi-objective optimization algorithm quantitatively), several performance indices can be adopted [T. Okabe et al., 2003]. Table 3 summarizes the performance indices used to assess the novel algorithm in searching optimal solutions for the test function considered (ZTD1), all the results obtained represent an average over 50 runs.

Table 3—Performance evaluations on ZTD1 test function (q = 0.5)

	Novel algorithm (q = 0.5)	MODE	MOGA	NSGA-II
Performance indices	Value	Value	Value	Value
execution time (s)	26.52	1.54	4.83	16.06
CPU time (s)	26.56	1.55	6.42	16.15
generational distance	1.25E-04	1.33E-05	5.81E-01	1.10E-02
inverted generational distance	9.86E-05	3.41E-07	5.38E-01	6.79E-03
spacing	5.10E-04	5.50E-04	1.29E-03	1.62E-03
distribution	5.02E-03	6.07E-03	7.44E-03	3.01E-03
spread	0.65303	0.70099	0.8121	0.4328
non-dominated solutions	199.2	185.66	195.58	200
fitness evaluations	100000	100200	na	na
identical non-dominated solutions	0	0	1.94	0

In Table 4, a sensitivity analysis of the novel algorithm performance to q = 0, q = 0.2 and q = 0.5 clearly demonstrates that it reaches the same performance shown by MODE in a reasonable time, thanks to a proper setting of q, making it a suitable candidate tool to be applied to the optimization of a hydrocarbon production system of Section 2. Particularly, the Pareto optimal front obtained (stars) compared with the true one (continuous line) of ZTD1 for the case q = 0 and q = 0.2 are shown in Figures 83 – 86, together with the corresponding convergence curves.

Table 4—Novel algorithm on ZTD1 test function with different mutation pressure values

	q = 0	q = 0.2	q = 0.5
Performance index	Value	Value	Value
execution time (s)	3.72	14.10	26.52
CPU time (s)	3.74	14.13	26.56
generational distance	1.98E-04	1.61E-04	1.25E-04
inverted generational distance	1.62E-04	1.34E-04	9.86E-05
spacing	4.53E-04	5.92E-04	5.10E-04
distribution	5.06E-03	5.10E-03	5.02E-03
spread	0.65101	0.66113	0.65303
non-dominated solutions	198.5	198.7	199.2
fitness evaluations	100000	100000	100000
identical non-dominated solutions	0	0	0

Description and Application of Equipment and Processes

We consider the surface production facilities of a hydrocarbon treatment plant, part of an oil and gas production system of Eni S.p.A., located in Italy. The treatment plant allows processing hydrocarbon fluids (i.e., raw oil) to obtain two main products, oil and gas, up to the requirements dictated by the market. In particular, gas is routed to the sales gas network, oil is sent to a nearby refinery, and water, a secondary product, is treated and, then, either re-injected or transferred by tracks. The plant consists in five interconnected treatment lines (see Figure 1), each one processing portion of all hydrocarbon fluids. On each line, various treatments are performed, among which the most relevant are:

- oil/gas separation;
- oil treatment;
- oil transport and storage;
- high-pressure and low pressure-gas compression;
- gas sweetening;
- gas dehydration;
- hydrocarbon dew-point control.

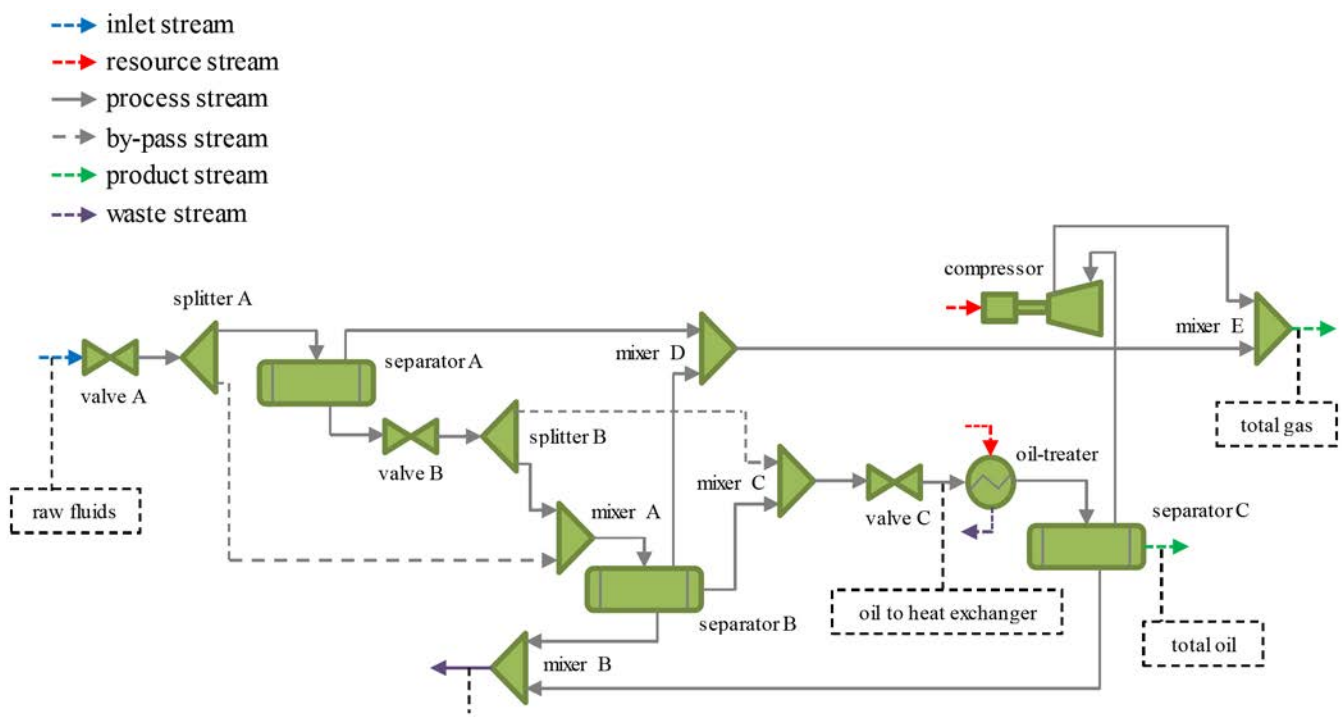

Figure 1—HYSYS model of the production system

Without loss of generality, Figure 1 shows the detailed sketch of a portion of a treatment line. Specifically, the raw fluids entering the plant are sent to the inlet separator, which has also the function of slug catcher, before being sent to the first three-phase separator (first-stage separator), generating an oil stream, sent with level-control to the second three-phase separator (second-stage separator), a high-pressure gas stream and a water stream, which is collected with other water streams of the plant and, then, sent to the oily water treatment unit. For the presented hydrocarbon treatment plant, at the exit of the first-stage separator, a shell-and-tube heat exchanger (oil-treater) is present in which oil, flowing in the tube side, is heated up through a water stream, flowing in the shell side and internally generated, aiming at increasing the temperature of the oil and, hence, facilitating its flow and liberating more gas from it, for gas production optimization. The gas separated in the second-stage separator is compressed in a centrifugal compressor up to the high-pressure level and, then, mixed with the other two streams coming from the inlet separator and the first-stage separator. The water stream is, thus, collected with other water streams and, then, sent away for further treatment.

A thermodynamic and, hence, exergy model of the line of Figure 2 has been developed to characterize the process in terms of the exergy efficiency, under the specific operational settings:

$$\bar{x} = \{\Delta P_{\text{valve A}},\ \Delta P_{\text{valve B}},\ P_{\text{separator C}},\ T_{\text{oil to heat exchanger}}\}:\quad \bar{x} \in D \subseteq R^4 \tag{14}$$

where $\bar{x}$ is a vector of optimization variables, particularly:

- $\Delta P_{\text{valve A}}$ is the pressure drop across the valve A;
- $\Delta P_{\text{valve B}}$ is the pressure drop across the valve B;
- $P_{\text{separator C}}$ is the pressure of the separator C;
- T_{oil} to heat exchanger is the temperature of the oil stream entering the heat exchanger.

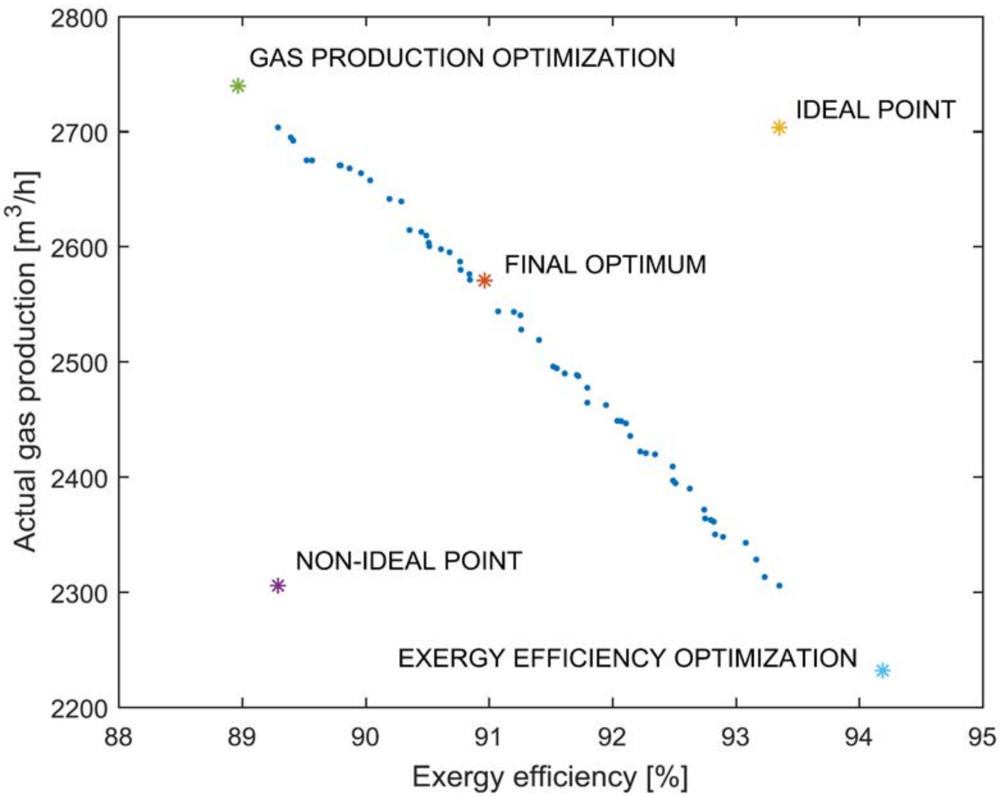

Figure 1—Pareto optimal front

These optimization variables are chosen because considered of major interest and commonly operated during the various operations of the oil and gas production plant, as directly accessible by the operator. Their allowed lower and upper bounds are listed in Table 5.

Table 5—Optimization variables

Optimization variable	Unit	Lower bound value	Upper bound value
$\Delta P_{valve\ A}$	[kPa]	50	300
$\Delta P_{valve\ B}$	[kPa]	50	300
$P_{separator\ C}$	[bar]	9.5	13.5
$T_{oil\ to\ heat\ exchanger}$	[°C]	50	80

The developed simulation provides the thermodynamic properties and the exergy values of each stream modelled, already accounting for the mixing effect, under the following assumptions:

- fixed flow rate and composition of raw oil;
- fixed pressure and vapor fraction of heating fluid;
- no by-pass and no product quality constraints (required by market specifications).

The composition of the raw oil entering the treatment section is reported in Table 6. The inlet stream is characterized by a temperature of 49.73 °C and a pressure of 33 bar, with a fixed molar flow rate equal to 1.115 kmole/s. The heating fluid (water), instead, is assumed to be at atmospheric pressure and with no vapor fraction. Neither by-pass is allowed in the investigated production plant, nor constraints are set, because we only focus on the first section of the treatment train and we neglect the specifications of the products outgoing the production plant and delivered to the market, respectively.

Table 6—Raw oil composition

Raw oil component	Molar fraction
N_2	0.015
CO_2	0.020
CH_4	0.557
C_2H_4	0.073
C3H8	0.043
i-C_4H_{10}	0.019
n-C_4H_{10}	0.020
i-C_5H_{12}	0.019
n-C_5H_{12}	0.010
benzene	0.017
toluene	0.124
H_2O	0.081
H_2S	0.002

The exergetic cost of a stream can be defined as the amount of exergy that has been consumed to produce the stream of the process [E. Querol et al., 2012]. The quantity of exergy consumed depends on both the performance of the units and the physical structure of the system; therefore, to reduce the exergetic cost and the consumption of resources it is possible to act on two fronts: improving the efficiency of the equipment or the physical structure of the system. These factors are associated with an increase in capital and operating costs, challenging the (already non-trivial) optimization, introducing thermoeconomic aspects into the thermodynamic optimization. In [E. Querol et al., 2012], a structured approach allows accounting for both exergetic cost and thermoeconomic cost analysis. In what follows, we consider:

- PEC_e as the Purchased Equipment Cost of the e-th piece of equipment;
- FC_e as the annual fixed cost flow of the e-th piece of equipment;
- $\dot{Z}e$ as the fixed cost flow of the e-th piece of equipment.

Indeed, as estimated based on operational manuals provided by Eni S.p.A. on the process plant under investigation, it has been possible to derive the main features of each equipment (e.g., type of equipment, size, capacity, materials, etc.). Summing all the purchased equipment cost values, we get the total Purchased Equipment Cost (PEC_{TOT}). From it, we can derive the Total Cost of Investment (TCI) using a proper value of Lang factor. Based on literature suggestion, a value of Lang factor equal to 3.63 has been adopted, being specific for solid-fluid process plants. To calculate the fixed cost flow of each piece of equipment, we need to calculate the annual fixed cost flow (FC_e), and divide it by the annual operating time (i.e., 8760 h/y). However, the annual fixed cost flow requires the definition of the total annual cost flow (FC_{TOT}), which is given as the sum of the annuity and the operating and maintenance costs. For the annuity, the recovery factor must be calculated starting from the interest rate, here set equal to 10 %. For the operation and maintenance costs, a value of the annual operation and maintenance cost per unit of capital invested equal to 1.4 % has been adopted. Once the total annual cost has been calculated, the annual fixed cost flow and the fixed cost flow can be determined, and the values for each piece of equipment are reported in Table 7.

Table 7—Equipment costs

Equipment	PEC_e [€]	FC_e [€/y]	$\dot{Z}_e$ [€/s]
valve A	0	0	0
valve B	0	0	0
valve C	0	0	0
separator A	6.50E+05	3.10E+05	9.84E-03
separator B	4.50E+05	2.15E+05	6.81E-03
separator C	3.30E+05	1.57E+05	4.99E-03
mixer B	0	0	0
mixer D	0	0	0
mixer E	0	0	0
oil-treater	4.40E+05	2.10E+05	6.66E-03
compressor	6.50E+05	3.10E+05	9.84E-03

The thermoeconomic costs of resources are taken from literature; indeed, for the raw oil a cost equal to 0.812 €/s is taken from [C. Sovrana, 2011], while for the compressor power a cost has been calculated as the product between the value of power and the electricity cost equal to 0.245 €/kWh, taken from [G. Cassetti et al., 2013]. Finally, for the heating fluid a cost per unit of mass equal to 0.0001 €/kg is taken from [E. Querol et al., 2012].

Presentation of Data and Results

Adopting the multi-objective optimization tool, we solve the optimization problem related to the case study of interest:

$$\overline{F}(\overline{x}) = \left(f_1(\overline{x}), f_2(\overline{x})\right) \in R^2 \tag{15}$$

where:

$$\overline{F}(\overline{x}) = \begin{cases} f_1(\overline{x}) = exergy \quad efficiency(\overline{x}) \\ f_2(\overline{x}) = gas \quad production(\overline{x}) \end{cases} \tag{16}$$

Denoting with $\dot{B}$ the exergy flow of a stream, we call:

- $\dot{B}in$ the exergy entering the system;
- $\dot{B}out$ the exergy exiting the system;
- $\dot{B}d$ the exergy destroyed by irreversible processes inside the system. Then,

$$f_1(\overline{x}) = \frac{\sum \dot{B}_{out}}{\sum \dot{B}_{in}} = \frac{\sum \dot{B}_{in} - \dot{B}_d}{\sum \dot{B}_{in}} = 1 - \frac{\dot{B}_d}{\sum \dot{B}_{in}} \tag{17}$$

$$f_2(\overline{x}) = \text{actual volume of total gas} \tag{18}$$

We set NP = 200 individuals and G_{MAX} = 100, and the remaining parameters as reported in Table 2.

Applying the TOPSIS technique, we get the unique final optimal solution, shown in Figure 2, in which the ideal and non-ideal points required to select it among all the non-dominated solutions obtained by the multi-objective evolutionary algorithm are also shown. The final optimal solution setting is reported in Table 8, that also lists the optimal solution settings that would have been collected if the problem was addressed in a single-objective manner with the in-house optimization tool (i.e., independently optimizing gas production and exergy efficiency).

Table 8—Optimal settings

		Multi-objective	Gas production	Exergy efficiency
Optimization variable	Unit	Value	Value	Value
$\Delta P_{valve\ A}$	[kPa]	300	300	50
$\Delta P_{valve\ B}$	[kPa]	213.7	300	50
$P_{separator\ C}$	[bar]	13.43	9.5	13.5
$T_{oil\ to\ heat\ exchanger}$	[°C]	50.40	80	50

The settings of Table 8 lead to the exergy efficiency and gas production of Table 9. The values of exergy inlet/outlet represent the sum of all exergy streams entering/exiting the system under investigation: hence, apart from the fixed exergy contribution given by the incoming raw oil, it accounts for the resources and the products, respectively; furthermore, the exergy efficiency refers to its ratio, whereas the gas production is the actual one outgoing the treating section under investigation. The power of the gas compressor and the rate of the heating fluid required are also given.

Table 9—Results

		Multi-objective	Gas production	Exergy efficiency
Model variable	Unit	Value	Value	Value
exergy inlet	[kW]	7270	7564	7285
exergy outlet	[kW]	6613	6729	6862
exergy efficiency	[%]	90.96	88.96	94.19
gas production	[m^3/h]	2571	2740	2232
compressor power	[kW]	35.65	118.9	59.11
heating fluid rate	[kg/s]	0.753	6.832	0.610

In Table 9, we notice that exergy efficiency and gas production for the multi-objective case are a trade-off of the values obtained with the single-objective cases. This is due to the fact that if we assume the hydrocarbon stream entering the production system at constant flow rate, composition and thermodynamic conditions, the exergy content of any hydrocarbon fluid entering the system is not involved in the optimization; whilst the exergy efficiency optimization is driven towards an optimal configuration having lower irreversibilities. Specifically, the improvement of the exergy efficiency of the plant, either in single- or multi-objective optimization, could be reached reducing the irreversibilities inside the system and reducing the irreversible conversion of resources, accordingly. Indeed, based on Equation 14 the maximization of the exergy efficiency implies reducing the irreversibilities, which also accounts for wastes and, hence, minimizing $$. To identify the equipment responsible for the largest irreversibility generation, we have proceeded apportioning the entire system exergy into the exergy destroyed by each piece of equipment, by calculating:

- the local efficiency of each piece of equipment;
- the exergy destroyed in each piece of equipment.

This assessment is a powerful way to identify the major sources of irreversibilities inside the system and consequently work to improve the thermodynamic performance. In Table 10 and 11 the local efficiency and the exergy destroyed by each piece of equipment are calculated, respectively.

Table 10—Local efficiency of each piece of equipment

Component	Multi-objective	Gas production	Exergy efficiency
valve A	97.54	97.54	99.61
separator A	96.60	96.60	96.64
valve B	98.36	97.67	99.66
separator B	93.57	95.36	94.43
mixer D	97.95	97.08	99.58
valve C	84.46	77.30	81.92
oil-treater	93.86	79.91	95.48
separator C	93.50	97.52	92.94
compressor	94.15	92.45	93.55
mixer E	99.95	99.66	99.91

Table 11—Exergy destroyed in each piece of equipment

Component	Multi-objective	Gas production	Exergy efficiency
valve A	177.164	177.164	28.2847
separator A	238.942	238.942	241.381
valve B	5.16910	7.34472	1.19218
separator B	15.8454	16.6739	15.4620
mixer D	133.037	189.893	27.6139
valve C	43.4214	61.4351	59.4538
oil-treater	16.1214	90.3813	13.1418
separator C	16.0184	8.91302	19.6145
compressor	7.71953	21.5182	11.5253
mixer E	3.53240	22.4773	5.74502

From Table 10, we notice that the optimization of the exergy efficiency of the whole system does not necessarily imply the best local optimization as well, but some pieces of equipment (e.g., the centrifugal compressor) show a higher local efficiency in the multi-objective optimization. Indeed, let us consider that if the exergy efficiency is optimized, the major contribution in its boosting is given by a reduction of exergy destroyed in equipment characterized by already high values of irreversibilities in the gas production case. However, when gas production and exergy efficiency are merged in a holistic and multidisciplinary way, two drivers guide the exploration towards the final optimal solution, which, in case of the centrifugal compressor, means an optimal configuration with lowest pressure ratio and, hence, highest local efficiency and lowest resource consumption, this latter shown in Table 13. Thus, these two features of the compressor clearly highlight a non-monotonic trend with gas production, but the attainment of a minimum/maximum, depending if we are considering the resources consumption or the local efficiency, respectively. Similar considerations can be done for the other pieces of equipment. Furthermore, apart from completely irreversible processes, such as throttling and mixing, the first most important equipment is the oil-treater, the weakest point in the model, with a local efficiency equal to 79,91 %. In the gas production optimization, hence, the oil-treater would require the major efforts to improve the overall process quality. In Table 12, several properties of the oil-treater (e.g., values of the heat flow ($$), the logarithmic mean temperature difference (LMTD) and the overall heat transfer coefficient multiplied by the exchanging area (U·A)) are given under the optimal operational settings found for the multi-objective and the single-objective (gas production and exergy efficiency) optimization.

Table 12—Oil-treater properties under the optimal operational settings found for the multi-objective and the single-objective (gas production and exergy efficiency) optimization.

Case	$\dot{Q}$ [kJ/h]	LMTD [°C]	UA [kJ/°C h]
gas production	4830399	14,02	344626
exergy efficiency	413367	24,89	16609
multi-objective	515844	24,77	20828

Thus, the increase of the oil-treater local efficiency in the multi-objective optimization is mainly given by a reduction of the heat flow exchanged and, consequently, a lower consumption of heating fluid. Therefore, a lower duty exchanged is translated in a lower value of UA, meaning that either a lower overall heat transfer coefficient is admitted or a smaller exchanging area is needed with the possibility to save on heat exchanger investment cost. Specifically, with respect to the gas production optimization, a local efficiency improvement of +19,5 % and of +17,5 % is attained by the oil-treater in the exergy efficiency optimization and in the multi-objective optimization, respectively. The second most important equipment is the gas compressor, whose best thermodynamic performance is achieved with the multi-objective optimization, strongly decreasing the exergy destroyed and, hence, reducing the useful work lost and not exploited due to irreversibilities. To better understand the actual thermodynamic reasons behind the gas compressor local efficiency boost, some properties (e.g., values of the gas compressor power (P_c), the compressor ratio (β) and the pressure difference between the discharge and the suction (ΔP_c)) are provided in Table 13.

Table 13—Compressor's cases

Case	P_c [MW]	β	Δp_c [kPa]
gas production	118.89	2.842	1750
exergy efficiency	59.11	2.370	1850
multi-objective	38.65	2.074	1443

Considering that the same value of compressor adiabatic efficiency equal to 75 % have been set for all the three cases, Table 13 shows a power consumption decrease of −50.29 % from the gas production optimization to the exergy efficiency one and a further −34.61 % is reached in the multi-objective optimization. The reason for this consumption saving derives from a decrease of compressor ratio, whereas the pressure difference does not show a characteristic trend as it depends on both the suction and discharge pressures, whose setting accounts for the overall optimization of process variables. For an insightful discussion on the results, the exergy analysis is here complemented with an exergetic and a thermoeconomic cost analysis because the exergy analysis, apart from describing the quality of any thermodynamic process, does not give any information about the costs of each system stream, which can be even more interesting and of practical application. Table 14 shows the thermoeconomic costs related to the resources consumed in the hydrocarbon production system for the different optimizations and the corresponding total profit attained, this latter calculated as the total revenues gained by selling the produced gas, net of all the production costs sustained in treating of hydrocarbons.

Table 14—Thermoeconomic cost of resources and total profit

		Multi-objective	Gas production	Exergy efficiency
Thermoeconomic cost	Unit	Value	Value	Value
compressor power	[€/d]	227.3	699.1	347.5
heating fluid rate	[€/d]	0.651	5.903	0.527
total profit	[€/s]	1.192	1.261	1.185

We observe that in the multi-objective optimization, even though the thermoeconomic cost of the heating fluid is slightly higher than the one obtained in the exergy efficiency optimization, this increase is far from being comparable (in terms of order of magnitude) with the thermoeconomic cost reduction of the compressor, which unexpectedly exhibits a value lower than the single-objective cases mainly due to a decrease of power consumption. The total profit gained is in between the ones obtained with the two single-objective optimizations: lower than the gas optimization one, due to a lower gas production, and higher than the exergy efficiency one, as production costs (TEC) have been significantly reduced. Interesting to notice that, when optimizing the only exergy efficiency its value strongly increases, leading to a lower irreversible conversion of resources, but this also implies a decrease of gas production, the main revenues driver, therefore, a lower total profit is obtained. Finally, based on the theory explained in [E. Querol et al., 2012], once exergy, exergetic cost and thermoeconomic cost values of each stream are available, it is possible to calculate some important key performance indicators to assess the good performance of a process plant in terms of costs, both exergetic and thermoeconomic, namely:

- unit exergetic cost k^*;
- unit thermoeconomic cost, c^*;
- unit exergoeconomic cost, $c=k^*\cdot c^*$.

The unit exergetic cost of a stream represents the exergetic cost per unit of exergy content, hence, it is a dimensionless quantity, whereas the unit thermoeconomic cost is the ratio between the thermoeconomic cost of a stream and its exergetic cost, so that expressed in €/kJ. Finally, the unit exergoeconomic cost of a stream represents the thermoeconomic cost required to get a unit of exergy and, hence, is simply given by the ratio between the thermoeconomic cost and the exergy content of the stream, expressed in €/kJ. Therefore, its minimization is of fundamental importance in the design optimization of any thermodynamic system [G. Cassetti et al., 2013]. In Table 15, the values of k* and c are calculated for the product streams only.

Table 15—Unit products costs

Case	k*	c
gas production optimization	1.124	1.275E-04
exergy efficiency optimization	1.062	1.245E-04
multi-objective optimization	1.099	1.290E-04

It is possible to observe how the unit exergetic cost k* decreases in cases where exergy efficiency is considered, either in single- or multi-objective optimization. A reduction of this indicator means lower resource consumption and lower irreversibilities, hence, a decrease of destroyed exergy in the production of a unit of exergy outgoing the thermodynamic system. More attention is required for the interpretation of the unit exergoeconomic cost c because, even though its highest value is attained with the multi-objective optimization, it does not necessarily imply worse performance. Indeed, to better explain this behaviour, we need to split it in all the terms contributing to its calculation, as in Table 16, where the sum of the exergetic cost (EXC), thermoeconomic cost (TEC) and exergy content (EX) of the main products (oil and gas) are reported:

Table 16—Exergetic (EXC), thermoeconomic cost (TEC) and exergy content (EX) of main products (oil and gas)

Case	EXC [kW]	TEC [€/s]	EX [kW]
gas production optimization	7564.2	0.8583	6729.5
exergy efficiency optimization	7285.3	0.8542	6861.9
multi-objective optimization	7269.9	0.8528	6612.9

The highest unit exergoeconomic cost obtained with the multi-objective optimization can be justified as follows: in spite of the lowest thermoeconomic cost of the products, the significant decrease of their exergy content leads to a consequential increase of c. The decrease of exergy content of both oil and gas does not affect the thermodynamic quality of the system, because the produced exergy of any oil and gas production system is not the main target, as it is not exploited in further thermodynamic processes, while reduction of irreversibilities and consumption of resources are (and have been) achieved by looking either at the unit exergetic cost or the exergetic cost, this latter being the lowest among all. It is now clear how the developed multi-objective optimization algorithm, merging gas production and exergy efficiency concepts, leads to substantial economic savings with respect to the other single-objective optimization cases. In particular, in terms of thermoeconomic cost, we could have savings equal to 477 €/d and savings equal to 120 €/d (with respect to gas production single-objective optimization and exergy efficiency single-objective optimization, respectively). This is a cornerstone as it demonstrates not only an efficiency boost, but a better management of economic resources by the innovative optimization methodology. Of course, as a lower gas production is attained, the total profit gained from gas sale is lower, and this could be the starting point of a further interesting application of the multi-objective optimization tool. Thus, the exergy analysis has been proved to be an accurate way of assessing which equipment is performing worse and preventively introducing corrective actions to ensure good thermodynamic performance of the system, supporting the decision process in the choice of maintenance operations. However, all this is still far from being enough if we want to deal with an optimization analysis, mainly because cost of resources, equipment and cost formation of products are still not considered. The need of a more general analysis to be carried out in economic terms is a priority. The thermoeconomic analysis, based on the theory of exergetic costs, seeks to contribute towards achieving this task. The results reported so far confirm the improved management of the process plant and its efficiency enhancement, without neglecting the main target of the oil and gas industries, that is production maximization. It is interesting to notice how the highest unit exergetic and thermoeconomic costs are collected downstream of the system, by the total gas and total oil streams, because of being the only products.

Conclusions

In this work, an exergy modelling has been embedded into a multi-objective optimization approach with application to a real Eni S.p.A hydrocarbon production system, achieving a novel optimal solution, whose operational setting guarantees improved management of processes and resources of the system. The improved exergy efficiency, the substantial thermoeconomic savings and the improved performance reached with respect to other methodologies of literature represent a cornerstone in the context of constantly striving for better exergy efficiency, which is a simple idea in theory but difficult to put into practice, as it requires us to improve the output of our industrial equipment while consuming less at the same time. The multi-objective optimization approach adopted gives excellent results especially if we consider the simplicity of its search engine. Its flexibility and robustness have been proved, highlighting its ability to even outperform some multi-objective optimization algorithms of literature. It represents a proper investment and innovation to take the next leap; furthermore, its straightforward simplicity allows its implementation to other multi-objective optimization problems and the procedure can be further developed to handle a large number of multiple objectives.

References

M. Aminyavari et al., 2016] M. Aminyavari, A. H. Mamaghani, A. Shirazi, B. Najafi, F. Rinaldi. Exergetic, economic, and environmental evaluations and multi-objective optimization of an internal-reforming SOFC-gas turbine cycle coupled with a Rankine cycle. In: *Applied Thermal Engineering* **108**, pp. 833–846, 2016.

B. V. Babu et al., 2007] B. V. Babu, A. M. Gujarathi, P. Katla, V. B. Laxmi. Strategies of multi-objective differential evolution (MODE) for optimization of adiabatic styrene reactor. In: *Proceedings of the international conference on emerging mechanical technology: macro to nano (EMTMN-2007)*, p. 243, 2007.

S. Bandyopadhyay et al., 2013] S. Bandyopadhyay, S. Saha, *Unsupervised classification: similarity measures, classical and metaheuristic approaches, and applications*. Springer Science & Business Media, 2012.

P. Baraldi et al., 2016] P. Baraldi, F. Cannarile, F. Di Maio, E. Zio. Hierarchical k-nearest neighbours classification and binary differential evolution for fault diagnostics of automotive bearings operating under variable conditions. In: *Engineering Applications of Artificial Intelligence* **55**, pp. 1–13, 2016.

BP Energy Outlook, 2017] *BP Energy Outlook*, 2017

G. Cassetti et al., 2013] G. Cassetti, E. Colombo. Minimization of local impact of energy systems through exergy analysis. *Energy conversion and management*, **76**, pp. 874–882, 2013.

L. Chambers, 1995] L. Chambers. Practical handbook of genetic algorithms: applications. Vol. I; *new frontiers* Vol. **II**, CRC Press, 1995.

K. Deb et al., 2002] A fast and elitist multi-objective genetic algorithm: NSGA-II. *IEEE transactions on evolutionary computation* **6.2**, pp. 182–197, 2002.

Q. Fan et al., 2015] Q. Fan, X. Yan. Differential evolution algorithm with self-adaptive strategy and control parameters for P-xylene oxidation process optimization. In: *Soft Computing* **19.5**, pp. 1363–1391, 2015.

Q. Fan et al., 2017] Q. Fan, W. Wang, X. Yan. Multi-objective differential evolution with performance-metric-based self-adaptive mutation operator for chemical and biochemical dynamic optimization problems. In: *Applied Soft Computing*, 2017.

D. E. Goldberg, 1989] D. E. Goldberg. *Genetic algorithms in search, optimization, and machine learning, 1989*. In: Reading: Addison-Wesley. 1989.

J. H. Holland, 1975] J. H. Holland. Adaptation in natural and artificial systems: an introductory analysis with application to biology. *Control and Artificial Intelligence*. MIT Press, 4-th edition.

J. Kennedy, 2011] J. Kennedy. JParticle swarm optimization. *Encyclopedia of machine learning*. Springer US, pp. 760–766, 2011.

A. Konak et al., 2006] A. Konak, D. W. Coit, A. E. Smith. Multi-objective optimization using genetic algorithms: A tutorial. *Reliability Engineering & System Safety*, **91.9**, pp. 992–1007, 2006.

T. Murata et al., 1995] T. Murata, H. Ishibuchi. MOGA: Multi-objective genetic algorithms. In: *Evolutionary Computation, 1995.*, *IEEE International Conference on*. Vol.**1**. IEEE, 1995.

T. Okabe et al., 2003] T. Okabe, Y. Jin, B. Sendhoff. A critical survey of performance indices for multi-objective optimization. In: *Evolutionary Computation, 2003. CEC'03*. The 2003 Congress on. Vol. **2**. IEEE, pp. 878–885, 2003.

E. Querol et al., 2012] E. Querol, B. Gonzalez-Regueral, J. L. Perez-Benedito. *Practical approach to exergy and thermoeconomic analyses of industrial processes*. Springer Science & Business Media, 2012.

T. Robič et al., 2005] T. Robič, B. Filipič. Differential evolution for multiobjective optimization. In: *Evolutionary multi-criterion optimization*. Springer Berlin/Heidelberg, pp. 520–533, 2005.

T. Sağ et al., 2016] T. Sağ, M. Çunkağ. A new ANC-based-multiobjective optimization algorithm with an improvement approach (IBMO: improved bee colony algorithm for multiobjective optimization). In: *Turkish Journal of Electrical Engineering & Computer Science* **24.4**, 2016.

S. Scaramellini et al., 2015] S. Scaramellini, P. Cerri, A. Bianco, S. Masi, *Eni S.p.A*. Short-term production management: continuous application of an innovative integrated production optimization tool. In: *SPE Annual Technical Conference and Exhibition*. Society of Petroleum Engineers, 2015.

S. Scaramellini et al., 2017] S. Scaramellini, P. Cerri, A. Bianco, S. Masi, *Eni S.p.A*. Energy efficiency boosting: field application of an innovative integrated production optimization tool to maximize production and save energy. In: Offshore Mediterranean Conference and Exhibition. Offshore Mediterranean Conference, 2017.

A. Seshadri, 2007] A. Seshadri. *A fast elitist multi-objective genetic algorithm: NSGA-II. Mathlab Central, file exchange, mathworks*, 2007.

C. Sovrana, 2011] C. Sovrana. *Speciale: conoscere meglio il petrolio*. 2011.

R. Storn et al., 1997] R. Storn, K. Price. Differential evolution – a simple and efficient heuristic for global optimization over continuous spaces. In: *Journal of global optimization*, pp. 341–359, 1997.

F. Verre et al., 2011] F. Verre, A. Casarotti, A. Palma, G. Viadana, *Eni E&P, OPSO Eni E&P*. Improving operations using model based decision support. In: Offshore Mediterranean Conference and Exhibition. Offshore Mediterranean Conference, 2011.

G. Viadana et al., 2012] G. Viadana, D. Albani, M. Distaso, A. Sharon, *eni e&p*. Integrated production optimization and surface facilities management through advanced optimization techniques. In: *SPE International Production and Operations Conference & Exhibition*. Society of Petroleum Engineers, 2012.

G. Viadana et al., 2013] G. Viadana, S. Masi, A. Sharon, M. Distaso, *eni e&p PROD dept.*, E. Zio, *Chair on Systems Science and Energetic Challenge, Ecole Centrale Paris and Supelec, Politecnico di Milano*. Integrated production optimization through model-based decision support and advanced optimization techniques. In: Offshore Mediterranean Conference and Exhibition. Offshore Mediterranean Conference, 2013